

EMMap: A Systematic Framework for Spatial EMFI Mapping and Fault Classification on Microcontrollers

Gandham Sai Santhosh
ee22b101@smail.iitm.ac.in
IIT Madras, India

Siddhartha Sanjay Naik
ns25z175@smail.iitm.ac.in
IIT Madras, India

Ritwik Badola
cs22s016@cse.iitm.ac.in
IIT Madras, India

Chester Rebeiro
chester@cse.iitm.ac.in
IIT Madras, India

Abstract—Electromagnetic Fault Injection (EMFI) is a powerful technique for inducing bit flips and instruction-level perturbations on microcontrollers, yet existing literature lacks a unified methodology for systematically mapping spatial sensitivity and classifying resulting fault behaviors. Building on insights from O’Flynn [1] and Kuhnappel [2] et al., we introduce a platform-agnostic framework for Spatial EMFI Mapping and Fault Classification, aimed at understanding how spatial probe position influences fault outcomes.

We present pilot experiments on three representative microcontroller targets including the Xtensa LX6 (ESP32) and two ChipWhisper boards not as definitive evaluations, but as illustrative demonstrations of how the proposed methodology can be applied in practice. These preliminary observations motivate a generalized and reproducible workflow that researchers can adopt when analyzing EMFI susceptibility across diverse embedded architectures.

Index Terms—Electromagnetic Fault Injection, EMFI, Fault attacks, Spatial mapping, Embedded security

I. INTRODUCTION

Electromagnetic Fault Injection (EMFI) has emerged as a practical and non-invasive technique for inducing transient faults in microcontrollers and system-on-chip (SoC) architectures. A carefully timed EM pulse can alter the execution path of a processor like skipping instructions, corrupting SRAM values, or bypassing security checks and thereby exposing subtle vulnerabilities in embedded systems. Prior studies have demonstrated this capability across architectures ranging from ARM microcontrollers to modern desktop-class processors. In particular, Kuhnappel [2] *et al.* show that EMFI can reliably modify control flow, escape loops, and corrupt data when the injected pulse is aligned with narrowly defined execution windows, often synchronized with bus-level or GPIO events. Their work further highlights that environmental conditions, such as lowering the SoC supply voltage, substantially increase the likelihood of successful injection.

Similarly, O’Flynn’s [1] investigation into EMFI parameter space reveals that fault behavior is strongly influenced by physical characteristics of the injection setup: reversing coil polarity changes the dominant bit-flip type, adjusting probe height modulates fault magnitude, and scanning across the surface of a chip reveals regions with markedly different susceptibility. These insights collectively emphasize that EMFI outcomes are neither random nor uniformly distributed; rather, they arise from an interplay between spatial coupling, timing precision, and physical configuration.

Despite these advances, existing literature provides no unified methodology for systematically mapping *where* on a chip faults can be induced and *what type* of fault behavior arises from each spatial location. Many EMFI demonstrations remain highly platform-specific, with experimental details that do not generalize well across architectures. As a result, EMFI research often lacks the precision and repeatability needed for scientific rigor, and security evaluations remain dependent on ad-hoc, trial-and-error fault campaigns. Our motivation in this work is threefold. First, to move beyond coarse observations (“a glitch happened”) toward fault campaigns that consistently trigger specific behaviors such as instruction skips or bit-flips, enabling meaningful classification rather than stochastic success. Second, to identify which physical regions of a microcontroller are susceptible to EMFI and to document these vulnerabilities in a reproducible manner, transforming EMFI from a black-box technique into a spatially informed process. Third, to provide defenders and system designers with a structured approach to analyzing EMFI resilience, enabling targeted protections based on realistic, empirically grounded fault models.

II. PROPOSED FRAMEWORK FOR SPATIAL EMFI MAPPING AND FAULT CLASSIFICATION

The objective of this work is to develop a systematic and device-independent methodology for *spatial* characterization of EMFI susceptibility on microcontrollers, and for structured classification of resulting fault behaviors. The framework is organized into three components: (1) spatial probing and parameter exploration, (2) architectural instrumentation and fault observability, and (3) behavioral fault classification. Together, these components enable repeatable experiments, comparison across platforms, and progressive refinement toward targeted fault triggering.

A. Spatial Probing and Parameter Exploration

Spatial EMFI mapping begins with controlled variation of the probe position across the surface of the target device. Independent of the commercial or custom EMFI toolchain used, the framework assumes the following capabilities:

- The die area (or package surface) is divided into a set of probe coordinates, typically arranged in a uniform grid. The resolution of the grid is not fixed; coarse scans are followed by finer scans around regions of interest.

- EMFI pulses must expose tunable parameters such as discharge voltage, pulse width, coil polarity, and probe height. Prior work shows that these parameters materially affect both magnitude and *type* of resulting faults.
- The injection must be aligned with predictable program or hardware events. This includes GPIO toggles, bus transactions, or cycle markers within the firmware. Precise timing is essential, as EMFI success is strongly coupled to narrow execution windows.

The outcome of this stage is a multi-dimensional parameter space describing how spatial position and pulse parameters relate to observable deviations, forming the basis for subsequent fault classification.

B. Architectural Instrumentation and Fault Observability

Since internal microarchitectural state is generally inaccessible on production MCUs, the framework requires explicit instrumentation at the firmware level to detect and differentiate fault outcomes. To maintain generality across architectures, we adopt simple but expressive observability mechanisms:

- Tight loops, counters, or instruction sequences whose nominal behavior is known and easily checked for skips or early exits.
- Small blocks of SRAM with fixed patterns or CRCs to detect data corruption without requiring full memory dumps.
- UART, GPIO signals, or debug interfaces that emit parseable markers for automated logging.

These allow the framework to detect instruction-level disturbances, transient SRAM corruptions, or system-level anomalies (e.g., hangs) independent of the specific microcontroller used.

C. Behavioral Fault Classification

The final component of the framework organizes observed deviations into a hierarchy of fault classes. This is crucial for both scientific rigor and security evaluation. We distinguish three primary classes:

- 1) **Control-flow faults:** instruction skips, altered loop bounds, premature exits, or incorrect branch outcomes.
- 2) **Data corruption faults:** bit-flips in sentinel memory regions, register perturbations, or multi-byte corruption patterns.
- 3) **System-level faults:** hangs, resets, peripheral misbehavior, or error-flag activation.

Faults collected across multiple spatial coordinates and pulse configurations are used to build a *spatial susceptibility map* of the device. These maps serve as empirical approximations of the underlying physical coupling between the EM field and microarchitectural structures.

This section summarizes how the proposed framework was instantiated on three representative microcontroller-class platforms. The goal of these experiments is not to provide exhaustive device characterization, but to demonstrate how each stage of the framework which is spatial probing, instrumentation, and fault classification can be operationalized in practice.

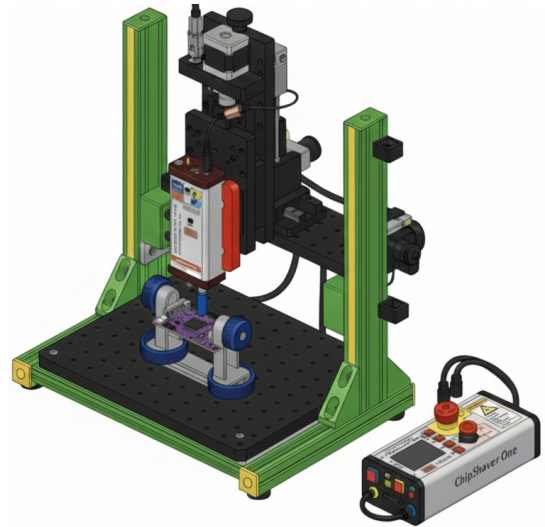


Fig. 1: CAD-style illustration of the EMFI setup used in this work, including the XYZ motion stage, ChipSHOUTER pulse generator, EMFI probe, 3D-printed target holder, and ESP32 target board.

D. Target Platforms

To exercise the framework across heterogeneous architectures, we selected three platforms with distinct levels of visibility into internal state:

- **Tensilica Xtensa LX6 (ESP32):** provides full debug access, enabling register snapshots and breakpoint-controlled execution. This allows fine-grained observation of control-flow and architectural state under EMFI.
- **ChipWhisperer CW521 (external SRAM target):** contains an off-chip memory region isolated from any processor. This enables direct observation of bit-level memory corruption without interference from pipelines or caches.
- **ChipWhisperer CW322 (STM32F3 MCU):** integrates CPU, SRAM, and peripherals on-die, representing a realistic embedded target where only high-level program behavior is observable.

Together, these platforms allow demonstration of the framework across scenarios ranging from high observability (ESP32) to highly constrained embedded conditions (CW322).

E. Spatial Scanning Configuration

Each platform was scanned using a uniform grid of spatial probe positions, with resolution chosen according to practical limits of probe movement and target form factor. Coarse grids were used to identify regions of elevated susceptibility, while finer grids were applied selectively around these regions for refinement. For each coordinate, multiple EMFI pulses were injected under a fixed set of pulse parameters to capture statistical behavior.

Consistent with prior reports, we observed that variation in coil polarity, probe height, and discharge parameters meaningfully affected the probability and type of observed deviations.

These variations are treated within the framework as part of the parameter-exploration stage rather than as fixed properties of any specific platform.

F. Firmware Instrumentation for Observability

Following the framework, each platform was instrumented with minimal but expressive observability mechanisms:

- **Xtensa LX6:** breakpoints were inserted within a reference program path. At each halt, register states (PC, general-purpose registers, and local disassembly) were captured automatically. This enabled distinguishing transient register disturbances from stable architectural behavior.
- **CW521:** memory patterns were written to the external SRAM, and full read-back comparisons were performed following injection. This allowed direct enumeration of bit-flip locations and magnitudes, serving as an illustrative example of physical data corruption mapping.
- **CW322:** firmware-level sentinel memory blocks with CRC checks were incorporated, along with deterministic loop counters that produced predictable control-flow markers. The resulting UART or GPIO outputs provided a lightweight means of detecting instruction skips, data corruption, or hangs.

These instrumentation mechanisms were selected to align with the framework requirements rather than to optimize results for any specific device.

G. Illustrative Observations

Across the three platforms, we observed representative instances of the fault classes defined in the framework:

- ESP32 occasionally halted with altered register states, and the STM32-based CW322 exhibited skipped loop iterations or premature exits.
- CW521 external SRAM showed localized bit flips under certain spatial and pulse configurations, consistent with expectations for an isolated memory device.
- Resets, hangs, or desynchronized UART outputs appeared on the MCU-based platforms under specific timing alignments.

To illustrate how spatial EMFI behavior manifests in practice, Fig. 2 summarizes representative outputs from the CW521 external-SRAM platform. The 2-D heatmap in Fig. 2(a) aggregates the total number of observed bit-flip events per probe coordinate across repeated injections. The resulting spatial gradient serves as a coarse susceptibility map: darker regions correspond to coordinates where no corruption was detected, whereas lighter regions highlight probe locations that consistently induced high-magnitude disturbances. Because CW521 exposes only memory-level effects, this visualization provides a direct spatial signature of physical coupling between the EM pulse and the SRAM array.

Fig. 2(b) complements this view by plotting a 3-D scatter of individual fault events, where each point encodes the (x, y) probe coordinate and the associated error count for a single trial. This representation makes the probabilistic nature of

EMFI readily visible. Points with similar spatial coordinates exhibit varying error magnitudes, reinforcing that even at a fixed location, the induced disturbance amplitude depends on micro-scale EM coupling, stochastic charge redistribution, and pulse-to-pulse variation. Together, these plots demonstrate that spatial position is a primary determinant of corruption density on the CW521 device and that repeated injections are necessary to correctly estimate susceptibility at any given coordinate.

These observations are preliminary and are included strictly to illustrate the application of the framework. No claims are made regarding completeness, reproducibility across all conditions, or device-specific vulnerability conclusions.

H. Role of These Demonstrations

The primary role of these demonstrations is to validate that the proposed framework can be applied to diverse microcontroller environments with varying observability constraints. The experiments provide qualitative evidence that:

- 1) spatial probe position has measurable impact on fault behavior,
- 2) simple firmware instrumentation is sufficient for high-level fault classification,
- 3) and the framework can organize observed behavior into coherent, cross-platform fault classes.

These findings motivate the more general discussion and systematization presented in the following section.

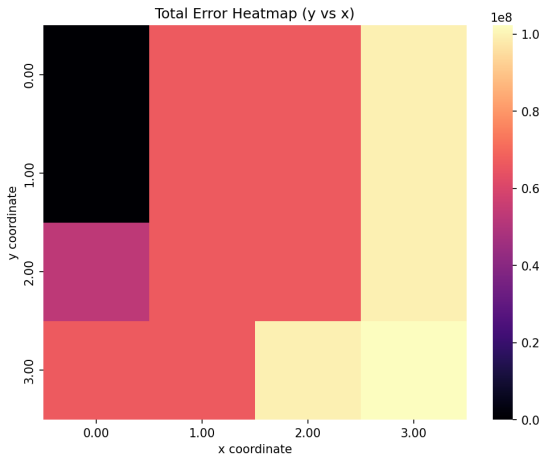
III. DISCUSSION: SYSTEMATIZING SPATIAL EMFI BEHAVIOR

The preliminary demonstrations across the three platforms highlight broader principles that underlie spatial EMFI behavior. Although each device differs in architecture, memory hierarchy, and observability, several consistent themes emerge when the framework is applied. This section systematizes these themes and articulates general insights that inform how spatial mapping and fault classification should be interpreted by practitioners.

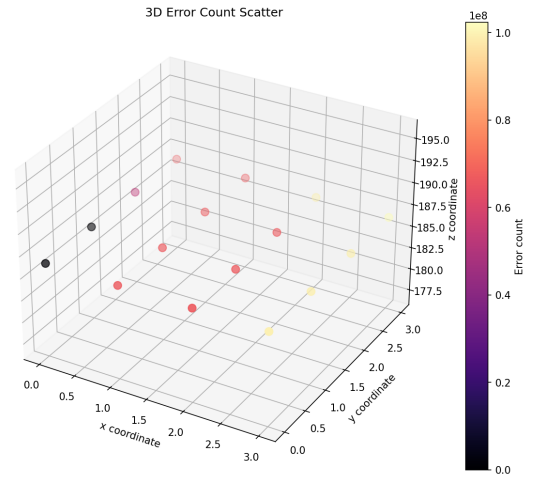
A. Spatial Sensitivity as a Fundamental Property

Prior work has clearly shown that EMFI susceptibility is not uniform across a chip surface. O’Flynn’s results demonstrate that even millimeter-scale movements of the probe can meaningfully alter both the likelihood and the type of induced faults. Similarly, Kuhnappel *et al.* observe that specific subregions of a large SoC exhibit markedly different behavior under identical pulse conditions.

Our demonstrations reinforce this principle: spatial position consistently influences whether the observed faults fall into control-flow, data-corruption, or system-level categories. Even when internal mapping (e.g., die layout or memory banks) is unknown, spatially organized sampling reveals meaningful gradients in susceptibility. The framework therefore treats spatial mapping as a first-class component, rather than a secondary tuning step.

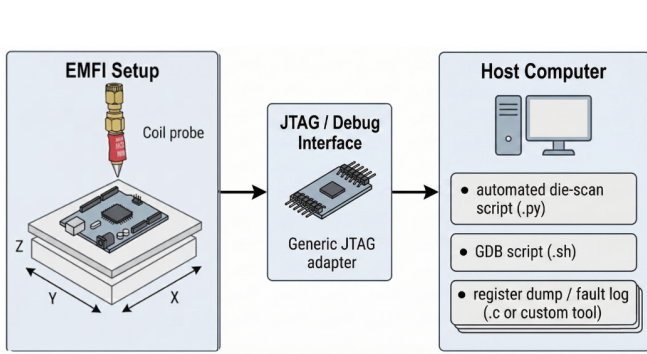


(a) 2-D error heatmap (per-coordinate error counts).

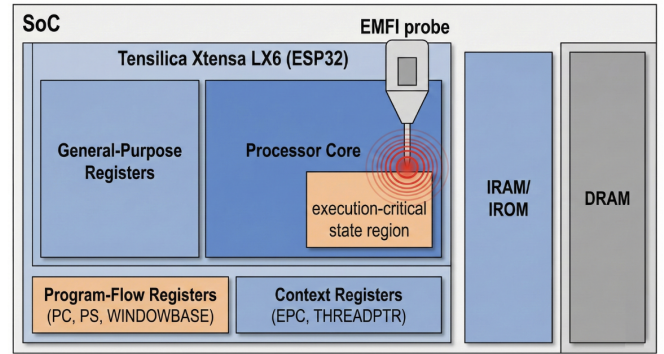


(b) 3-D scatter (x, y, error count / repeat index).

Fig. 2: Representative CW521 outputs: heatmap and 3D error scatter from pilot runs.



(a) Pipeline for spatial EMFI experimentation showing the probe setup, JTAG interface, and automated host-side tooling.



(b) Conceptual diagram of EMFI interaction with the Xtensa LX6 core, highlighting the execution-critical state region.

Fig. 3: Visual Overview of Fault Injection Analysis on Xtensa LX6 (ESP32)

B. Timing Precision Remains a Critical Axis

Across all platforms, the success of injection attempts depended strongly on temporal alignment between the EM pulse and specific execution windows. This aligns with prior observations that only narrow timing margins around instruction fetch, memory read, or pipeline transitions produce reliable disturbances.

While the demonstrations in this work employ basic timing markers (e.g., GPIO toggles or loop cycles), the framework is compatible with higher-precision tools such as FPGA-based delay generators or bus-triggered injection. Importantly, the necessity for temporal precision is treated as architecture-independent: any microcontroller with deterministic execution sequences can serve as a substrate for repeatable timing-aligned fault campaigns.

C. Physical Parameters as Fault-Mode Modulators

The EMFI parameter space is multidimensional. Coil polarity, probe height, discharge voltage, pulse width, and local EM coupling all have nontrivial influence on fault outcomes.

O’Flynn’s observations that reversing coil polarity shifts the dominant bit-flip direction and that reducing probe height increases fault magnitude were reflected qualitatively across our experimental platforms.

Within the framework, these parameters are not treated as fixed experimental constants. Instead, they serve as *fault-mode modulators* that help distinguish whether observed phenomena arise from localized memory disturbance, timing violations, or system-level perturbations. This classification supports reproducibility without requiring exact replication of hardware conditions.

D. Classification Enables Structured Interpretation

The framework’s three-tier classification scheme: control-flow faults, data-corruption faults, and system-level faults proved expressive enough to organize all observed deviations, despite the differences among platforms. This validates that the taxonomy is practical and sufficiently agnostic to architectural details.

The distinction is especially important for MCU-class devices where internal state visibility is limited. For example, a skipped loop iteration and a CRC mismatch may appear superficially similar but arise from fundamentally different microarchitectural effects. By categorizing these faults separately, the framework enables more meaningful cross-platform comparisons and supports clearer reasoning about underlying mechanisms.

E. Toward a Generalized Methodology

The combination of spatial sensitivity, temporal precision, and physical modulation suggests that a generalized EMFI mapping methodology should begin with coarse spatial scans to identify broad susceptibility regions, employ lightweight instrumentation to distinguish fault classes, iteratively refine both spatial resolution and pulse parameters, and interpret observations through the lens of architecture-independent principles rather than device-specific heuristics.

F. Limitations and Scope

As with all preliminary studies, the demonstrations presented here serve primarily to validate the *applicability* of the framework rather than to characterize any particular device. The results are intentionally conservative: no claims are made regarding completeness, exact spatial correspondence to die structures, or vulnerability of the tested platforms. Instead, the value lies in showing that the framework can structure experimentation in a principled and architecture-agnostic manner.

These limitations outline a natural direction for future work, where more precise timing instrumentation, physical die imaging, or higher-resolution spatial scans may yield deeper insights into the physical origins of observed behaviors.

IV. PRACTICAL GUIDELINES FOR APPLYING THE FRAMEWORK

While the previous sections define the conceptual structure of the framework, effective use in real EMFI campaigns requires concrete experimental practices. The following guidelines consolidate lessons from prior literature and our illustrative demonstrations into a set of practical recommendations for researchers and evaluators.

A. Timing Alignment and Triggering

EMFI effectiveness is strongly dependent on alignment with specific execution windows. To maximize interpretability:

- **Use deterministic firmware markers:** GPIO toggles, loop iteration points, or UART tokens provide coarse alignment without relying on internal debug hardware.
- **Favor narrow windows:** even simple time-offset sweeps can reveal windows of heightened vulnerability, consistent with prior observations that many faults require precise synchronization.
- **Record timing offsets explicitly:** timestamps, trigger delays, and event markers should be captured for each injection to support later analysis.

Accurate timing metadata allows researchers to correlate spatial and temporal effects more reliably.

B. Firmware Instrumentation for Observability

Because most microcontrollers do not expose internal state, firmware instrumentation is crucial:

- **Employ sentinel memory regions:** checksums or fixed patterns provide fast, lightweight detection of data corruption.
- **Use predictable control-flow constructs:** tight loops, constant-iteration counters, and simple arithmetic blocks make instruction skips immediately observable.
- **Generate structured output:** unambiguous UART or GPIO messages (e.g., `CF_SKIP`, `CRC_ERR`) facilitate automated logging and classification.

C. Fault Classification Workflow

To maintain consistent interpretation across devices:

- 1) Determine whether the deviation corresponds to control-flow, data corruption, or system-level behavior.
- 2) Measure loop iteration counts, bit-flip density, or reset patterns to gain deeper insight.
- 3) EMFI is probabilistic; classification should be based on repeated trials under identical parameters.

D. Reproducibility and Documentation Practices

To support scientific rigor, the following practices are recommended:

- Probe geometry, pulse parameters, timing offsets, and firmware versions should be logged for every experiment.
- Structured logs and repeatable scan sequences reduce manual error.
- Supply voltage, temperature, and noise sources can influence outcomes and should be documented when relevant.

E. Extensibility Toward Advanced Analysis

The framework is compatible with more sophisticated techniques when needed:

- **High-resolution timing:** FPGA- or logic-analyzer-based triggering can reveal finer-grained vulnerability windows.
- **Die-level spatial correlation:** microscopy or decapsulation allows aligning susceptibility maps with physical structures, as demonstrated in prior work on large SoCs.
- **Automated parameter search:** scripted sweeps of spatial, temporal, or pulse parameters can accelerate exploration of the fault space.

Overall, these guidelines operationalize the framework in a manner that is reproducible, device-agnostic, and compatible with EMFI infrastructure.

V. CONCLUSION

This work presents a systematic, platform-agnostic framework for spatial EMFI mapping and fault classification on microcontrollers. Motivated by the need for precision, repeatability, and scientific rigor in EMFI experimentation, the framework unifies spatial probing, firmware-level instrumentation,

and structured fault classification into a coherent methodology. Rather than focusing on device-specific vulnerabilities, the approach emphasizes general principles that hold across architectures: spatial susceptibility gradients, narrow timing windows for effective injection, and the modulatory influence of physical parameters such as coil polarity and probe height.

Pilot demonstrations on the Xtensa LX6 (ESP32) and two ChipWhisperer-based educational targets illustrate how the methodology can be instantiated under varying levels of observability. These experiments serve not as comprehensive evaluations but as practical examples of how the framework organizes EMFI behavior into interpretable categories and highlights the interplay between spatial, temporal, and physical dimensions.

By formalizing this workflow, the framework provides a foundation for reproducible EMFI research and offers a structured path for analysts seeking to characterize the fault-injection susceptibility of embedded systems. It also supports a more transparent and disciplined approach to security evaluation, enabling designers to reason about EMFI resilience using empirically grounded fault models.

Future extensions may incorporate high-resolution timing control, die-level imaging for spatial correlation, or automated multi-parameter exploration. Nonetheless, the core methodology presented here establishes a generalizable and extensible basis for advancing spatial EMFI characterization across diverse microcontroller platforms.

REFERENCES

- [1] C. O'Flynn, "NAEAN0011: Electromagnetic Fault Injection (EMFI) for Automotive Safety & Security Testing with ChipSHOUTER®," NewAE Technology, Tech. Rep., 2020. Available: https://media.newae.com/appnotes/NAE0011_Whitepaper_EMFI_For_Automotive_Safety_Security_Testing.pdf.
- [2] N. Kühnapfel, R. Bühren, H.-N. Jacob, T. Krachenfels, C. Werling, J.-P. Seifert, "EM-Fault It Yourself: Building a Replicable EMFI Setup for Desktop and Server Hardware," PAINE / arXiv preprint, Sept. 2022. Available: <https://arxiv.org/abs/2209.09835>.
- [3] NewAE Technology Inc., "CHIPSHOUTER® USER MANUAL," Feb 25, 2021. Available: https://media.newae.com/manuals/ChipSHOUTER_PRESS_1.3.pdf.
- [4] A. Cui and R. Housley, "BADFET: Defeating Modern Secure Boot Using Second-Order Pulsed Electromagnetic Fault Injection," WOOT (USENIX Workshop on Offensive Technologies), 2017. Available: <https://www.usenix.org/system/files/conference/woot17/woot17-paper-cui.pdf>.
- [5] N. Moro, A. Dehbaoui, K. Heydemann, B. Robisson, E. Encrenaz, "Electromagnetic Fault Injection: Towards a Fault Model on a 32-bit Microcontroller," arXiv / FDTC papers, 2014. Available: <https://arxiv.org/pdf/1402.6421.pdf>.
- [6] T. Troughkine, G. Bouffard, J. Clédière, "EM Fault Model Characterization on SoCs: From Different Architectures to the Same Fault Model," FDTC (Workshop on Fault Detection and Tolerance in Cryptography), 2021. Available: https://thomas.troughkine.com/assets/pdf/fdct_2021.pdf.
- [7] H. Liao and C. Gebotys, "Methodology for EM Fault Injection: Charge-based Fault Model," DATE (Design, Automation and Test in Europe), 2019. Available: <https://past.date-conference.com/proceedings-archive/2019/DATA/401.pdf>.
- [8] K. M. Abdellatif and O. Hériveaux, "SiliconToaster: A Cheap and Programmable EM Injector for Extracting Secrets," FDTC Workshop (FDTC/2020), 2020. Available: <https://fdtc.deib.polimi.it/FDTC20/shared/Abdellatif.pdf>.
- [9] J. Balasch, D. Arumí, S. Manich, "Design and validation of a platform for electromagnetic fault injection," DCIS (Design of Circuits and Integrated Systems), 2017. Available (PDF): https://www.researchgate.net/publication/323823120_Design_and_validation_of_a_platform_for_electromagnetic_fault_injection.
- [10] J. Toulemon, N. Ouldei-Tebina, J.-M. Galliére, P. Nouet, E. Bourbao, P. Maurine, "A Simple Protocol to Compare EMFI Platforms," IACR Cryptology ePrint Archive, 2020 (eprint). Available: <https://eprint.iacr.org/2020/1277.pdf>.
- [11] R. Bühren, H.-N. Jacob, T. Krachenfels, J.-P. Seifert, "One Glitch to Rule Them All: Fault Injection Attacks Against AMD's Secure Encrypted Virtualization," ACM CCS (preprint / arXiv), 2021. Available: <https://arxiv.org/abs/2108.04575>.
- [12] Y. Kim, R. Daly, J. Kim, C. Fallin, J. H. Lee, D. Lee, C. Wilkerson, K. Lai, O. Mutlu, "Flipping Bits in Memory Without Accessing Them: An Experimental Study of DRAM Disturbance Errors," ISCA, 2014. Available: https://people.inf.ethz.ch/omutlu/pub/rowhammer_isca2014.pdf.
- [13] J.-M. Dutertre, T. Riom, O. Potin, J.-B. Rigaud, "Experimental Analysis of the Laser-Induced Instruction Skip Fault Model," NordSec / Microelectronics Reliability (2019/2021 versions), 2019. Available (paper / slides): <https://hal.science/hal-02420090/document>.
- [14] S. Delarea and Y. Oren, "Practical, Low-Cost Fault Injection Attacks on Personal Smart Devices," Applied Sciences, vol. 12, no. 1, 2022. Available: <https://www.mdpi.com/2076-3417/12/1/417>.
- [15] SiliconToaster / authors, "SiliconToaster project materials (FDTC paper + code)," 2020. Available: <https://fdtc.deib.polimi.it/FDTC20/shared/Abdellatif.pdf>.
- [16] Riscure, "Riscure EM Probe Station 5 (datasheet) / EM-FI Transient Probe," product datasheet. Available: <https://getquote.riscure.com/picdb/filedb/3792/EMPS%205%20datasheet.pdf>.
- [17] T. Troughkine, G. Bouffard, J. Clédière, "EM Fault Model Characterization on SoCs: From Different Architectures to the Same Fault Model," FDTC 2021 (paper). Available: https://thomas.troughkine.com/assets/pdf/fdct_2021.pdf.
- [18] H. Liao and C. Gebotys, "Methodology for EM Fault Injection: Charge-based Fault Model," DATE 2019 proceedings (paper), 2019. Available: <https://past.date-conference.com/proceedings-archive/2019/DATA/401.pdf>.
- [19] Z. Chen, G. Vasilakis, K. Murdock, E. Dean, D. Oswald, F. D. Garcia, "VoltPillager: Hardware-based fault injection attacks against Intel SGX Enclaves using the SVID voltage scaling interface," USENIX Security 2021 (paper). Available: <https://www.usenix.org/conference/usenixsecurity21/presentation/chen-zitai>.
- [20] Z. Kenjar, T. Frassetto, D. Gens, M. Franz, A.-R. Sadeghi, "VOLTpwn: Attacking x86 Processor Integrity from Software," USENIX Security 2020. Available: <https://www.usenix.org/conference/usenixsecurity20/presentation/kenjar>.
- [21] P. Qiu, D. Wang, Y. Lyu, R. Tian, C. Wang, G. Qu, "VoltJockey: A New Dynamic Voltage Scaling based Fault Injection Attack on Intel SGX," IEEE Transactions on CAD (2020). Available: <https://ieeexplore.ieee.org/document/9083976>.
- [22] NewAE Technology, "ChipSHOUTER (GitHub repository)," NewAE / ChipSHOUTER project page. Available: <https://github.com/newaetech/ChipSHOUTER>.